Modeling and Characterization of Metal-Semiconductor-Metal-based Source-Drain Contacts for Design and Robust Implementation of *a*-GaInZnO TFTs

Sangwon Lee[1], Kichan Jeon[1], Jun-Hyun Park[1], Yong Woo Jeon[1], Changjung Kim[2], Ihun Song[2], Jaechul Park[2], Sunil Kim[2], Sangwook Kim[2], Youngsoo Park[2], Dae Hwan Kim[1], and Dong Myong Kim[1,a)]

[1]School of Electrical Engineering, Kookmin University, 861-1, Jeongneung-dong, Seongbuk-gu, Seoul, 136-702, KOREA [a)]dmkim@kookmin.ac.kr

[2]Semiconductor Laboratory, Samsung Advanced Institute of Technology, Nongseo-Dong, Giheung-Gu, Yongin-Si, Gyeonggi-Do, 446-712, KOREA

Abstract

Modeling and characterization of current-voltage characteristics of metal-semiconductor-metal (MSM) structure in amorphous GaInZnO (*a*-GIZO) FETs is very important for design, fabrication, and application to transparent flexible TFT integrated circuits. In this work, the gate voltage-dependent contact resistance in *a*-GIZO is semi-empirically modeled and experimentally extracted from external load resistor connected to source terminal with a suitable range of impedance. Because *a*-GIZO FETs inevitably contain an MSM structure, they consist of two metal-semiconductor (MS) contacts and one resistor between them. Proposed semi-empirical model of *a*-GIZO MSM structure includes a thermionic field emission current component and trap assisted band-to-band generation under reverse bias. The results calculated with proposed model agree well with experimental results from *a*-GIZO TFTs.

I. Introduction

In recent years, *a*-GIZO has been recognized and under active research as an attractive channel material for transparent thin-film transistors (TFTs). It provides high mobility and good transparency, as well as a low-temperature process that allows the fabrication of TFTs and circuits on flexible substrates such as plastics [1-3]. The characterization of contact properties between source/drain metal and the *a*-GIZO semiconductor is important because a high series resistance in source/drain contacts is a primary cause of the current crowding and performance degradation, wherein accumulated electron flows directly impact the electrical properties of TFTs, such as threshold voltage, mobility, I_{on}/I_{off} ratio, and sub-threshold swing.

a-GIZO FETs composed of two Schottky contacts [4] connected back to back in series with a semiconductor having a resistance. The current mechanism in MSM structure-based *a*-GIZO oxide-semiconductors is modeled by thermionic field emission (TFE) [5], trap-assisted generation [6] and thermionic emission (TE) [7] in Metal-S/D contacts, and the operation of the resistor in the *a*-GIZO channel layer.

In this work, a semi-empirical model of MSM structure for the Source-Drain contacts is proposed and characterized electrical properties between the channel layer and S/D metal contacts for robust design and assessment of *a*-GIZO TFTs.

II. Device Structure and I-V Characteristics

A schematic cross-section of integrated *a*-GIZO TFT is shown in Fig. 1 and has the most commonly used back-channel-etch staggered bottom gate structure for active-matrix liquid crystal displays (AMLCDs) and/or active-matrix organic-light-emitting-diode (AMOLED) displays. Devices are fabricated as follows: On a thermally grown SiO_2/Si substrate, the first sputtered deposition at RT and patterning of molybdenum (Mo) gate are followed by plasma-enhanced chemical vapor deposition (PECVD) of SiO_2 (100 nm) at 300 ºC. An active layer (Ga_2O_3:In_2O_3:ZnO=2:2:1 at %) is then sputtered by RF magnetron sputtering at RT in a mixed Ar/O_2 (100:1 at sccm) and wet-etched with diluted HF to get T_{IGZO}=70 nm. For the source/drain (S/D), a 200-nm-thick layer of Mo is sputtered at RT and then patterned by dry-etching. After N_2O plasma treatment on the channel surface of the IGZO active layer, a SiO_2 passivation layer is continuously deposited at 150 ºC by PECVD without a vacuum break. All the samples were finally annealed for 1 hr in the furnace at 250 °C. The channel length (L), the channel width (W), and the length of the overlap region between the gate and S/D (L_{ov}) are designed to be 2, 50, 200 μm, respectively. An amorphous phase of the fabricated *a*-GIZO layer was confirmed by XRD and TEM. And both transfer and output characteristics of the fabricated *a*-GIZO are shown in Fig. 2.

III. Modeling of S/D Contacts in *a*-GIZO TFTs

The contact resistance can be extracted by using the modified external loading method [8]. An external load resistor with a suitable range of impedance is connected to the source terminal. The total resistance is composed of external load resistance (R_L), source resistance (R_S), drain resistance (R_D), and channel resistance. The drain-current in the linear region of TFT operation is given by

$$I_{DS} = K\{V_{GS} - I_{DS}(R_S + R_L)V_T - 0.5[V_{DS} - I_{DS}(R_S + R_D + R_L)]\} \times [V_{DS} - I_{DS}(R_S + R_D + R_L)] \quad (1)$$

where K=(W/L)μC_{ox}, W=the channel width, L=the channel length, μ=the channel carrier mobility, and C_{ox}=the effective gate capacitance per unit area. Rearranging Eq. (1), we obtain

$$\frac{1}{I_{DS}} = \frac{R_L + R_S + R_D}{V_{DS}} + \frac{1}{K(V_{GS} - V_T - 0.5V_{DS})V_{DS}}. \quad (2)$$

By plotting $1/I_{DS}$ versus R_L with V_{GS} as a parameter, the x-axis intersection R_{L0} can be described as

$$-R_{L0}(V_{GS}) = R_S + R_D + \frac{1}{K(V_{GS} - V_T - 0.5V_{DS})}. \quad (3)$$

By plotting the V_{GS}-dependent $-R_{L0}$ versus $1/(V_{GS}-V_T-0.5V_{DS})^{-1}$, the contact resistance(R_C=R_S+R_D) on the source and drain can be extracted.

Under low bias condition, the generation current in the space charge region is expected to be the main component whereas the thermionic field emission current is dominant current component in the total current from the experimental results. The equivalent circuit model and the energy band diagram schematically explaining the overall current mechanisms in MSM structures are shown in Fig. 3. Following the Kirchhoff's laws in the S/D MSM structure, we obtain

$$I_{DS} = I_{R,Schottky} = I_{GIZO} = I_{F,Schottky} \quad (4)$$

$$V_{DS} = V_{R,Schottky} + V_{GIZO} + V_{F,Schottky} \quad (5)$$

$$V_{R,Schottky} \approx V_{R,Schottky} + V_{F,Schottky}. \quad (6)$$

Current in the MSM structure for the S/D contact is limited by the reverse biased Schottky contact and there are mainly three current components (J_{gen}, J_{TFE}, J_S in Eqs. (7)-(12)). Current on the reverse-biased side of the MS contact due to the trap assisted generation mechanism (J_{gen}) is originated from the thermally generated ehp's through the traps in the space charge region of S/D contacts in the *a*-GIZO channel layer. Adopting a characteristic parameter α in Eq. (8), we empirically modeled J_{gen} to match with experimentally observed current. On the other hand, the TFE current component in Eq. (9) is formed by the tunneling as electrons at the Fermi level are excited by thermal energy and transmitted through the Schottky barrier from the metal to the *a*-GIZO channel layer. And, another current in the MS contact is due to the TE component formed by electrons excited by the thermal energy overcoming the SB from the metal to the *a*-GIZO channel layer. Dominant current mechanisms across the MSM structure are expected to be TFE and trap-assisted generation mechanisms under reverse bias. These components with empirically extracted characteristic model parameters can be described by following models;

$$J_{R,Schottky} = J_{gen} + J_{TFE} + J_S \cong J_{gen} + J_{TFE} \quad (7)$$

$$J_{gen} = \frac{qn_i}{2\tau_0}\sqrt{\frac{2\varepsilon_{GIZO}}{qN_{sub}}\left(V_{bi} + V_{R,Schottky}\right)}\left[1 - \exp\left(\frac{V_{R,Schottky}}{V_{th}}\right)\right] \approx \alpha\sqrt{1 + \frac{V_{R,Schottky}}{V_{bi}}}\left[1 - \exp\left(\frac{V_{R,Schottky}}{V_{th}}\right)\right] \quad (8)$$

$$J_{TFE} = J_{TFE0} \exp\left(-\frac{qV_{R,Schottky}}{\varepsilon'}\right) \quad (9)$$

$$\varepsilon' = E_{00}\left[\frac{E_{00}}{kT} - \tanh\left(\frac{E_{00}}{kT}\right)\right] : \text{Characteristic energy} \quad (10)$$

$$J_{TFE0} = \frac{A^{*}T^{2}\sqrt{\pi E_{00}}}{kT}\sqrt{-qV + \frac{E_B}{\cosh\left(E_{00}/kT\right)}}\exp\left(-\frac{E_B}{E_0}\right) \quad (11)$$

$$E_0 = E_{00}\coth\left(E_{00}/kT\right), \quad E_{00} = \frac{\hbar}{2}\sqrt{\frac{N_{sub}}{m_{GIZO} * \varepsilon_{GIZO}}} \quad (12)$$

where n_i, τ_0, ε_{GIZO}, N_{sub}, V_{bi}, α, k, T, A^*, E_B, $\hbar$, and m_{GIZO}^* are the intrinsic carrier concentration, lifetime, the permittivity of *a*-GIZO, the body doping concentration, the built-in voltage, an empirical fitting parameter for the generation current component, the Boltzmann constant, the absolute temperature, the Richardson constant, a Schottky barrier height, the Planck constant, and the effective mass of electrons in the *a*-GIZO layer. E_0 and E_{00} are characteristic energy for the thermionic field emission current component.

IV. Experimental Characterization of *a*-GIZO TFTs

Fig. 4 shows I_{DS}-V_{DS} curves when the gate electrode is floated and the gate voltage is at 0V. In the linear mode of operation (V_{DS}=0.15V), the total resistances from two I_{DS}-V_{DS} curves is almost the same as $R_{T,gate_floating}$=121 [kΩ] and $R_{T,VGS=0V}$=132 [kΩ]. We propose a semi-empirical model employing R_C and R_{ch} when the gate voltage is at 0V. Voltage drop in the channel and contact region is calculated considering the extracted resistance from experimental results as shown in Fig. 5. The results calculated with our model reproduce the experimental results. The gate voltage dependent contact resistance for TFTs with W/L=200 μm/2 μm is extracted by the modified external loading method from Fig. 6. Contact resistance is extracted to be R_C=42.58 [kΩ] when the gate bias V_{GS} is zero. The I_{DS} vs. $\sqrt{V_{DS}}$ and log(I_{DS}) vs. V_{DS} curves for modeling and characterization of J_{gen} and J_{TFE} in the MSM structure are shown in Fig. 7. Experimental I-V curve agrees well with the empirical model. Finally, Fig.8 comparatively shows the measured I_{DS} -V_{DS} characteristics of *a*-GIZO MSM structure with I-V data from the semi-empirical model. Extracted model parameters are summarized in Table I.

V. Conclusions

A semi-empirical model based on the analytical current model combined with experimental I-V data is proposed for modeling and characterization of S/D MSM contacts in *a*-GIZO TFTs. Measured I_{DS}-V_{DS} characteristics of *a*-GIZO MSM structure are compared with the model and verified a good agreement. This result is expected to be useful in the design, modeling, and robust implementation of *a*-GIZO TFTs for transparent and flexible display applications.

Acknowledgements

This work is supported by research fund from Samsung Advanced Institute of Technology.

References

[1] K. Nomura *et al*., *Nature*, **432**, 488, 2004.
[2] H. Yabuta et al., *Appl. Phys. Lett.*,**89**, 112123, 2006.
[3] M. Kim et al., *Appl. Phys. Lett.*, **90**, 212114, 2007.
[4] E. H. Rhoderick, *Metal-Semiconductor Contact*, Oxford Science, 1980.
[5] F. A. Padovani and R.Stratton, *Solid-State Electronics*, **9**, 695, 1996.
[6] S. W. Kim et al., *Microelectronics Reliability* ,**48**, 382, 2008.
[7] S. M. Sze, *Physics of Semiconductor Devices*, 2nd ed, Wiley, New York, 1981.
[8] B.-Y. Tsui et al., *IEEE Electron Device Lett*., **29**, 1053, 2008.

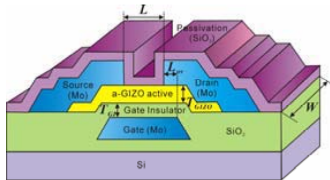

Fig. 1. Schematic structure of fabricated *a*-GIZO TFTs.

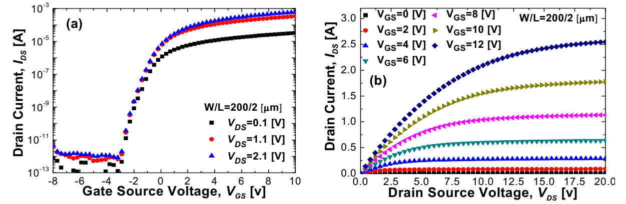

Fig. 2. (a) Measured transfer characteristics and (b) output characteristics of *a*-GIZO TFTs.

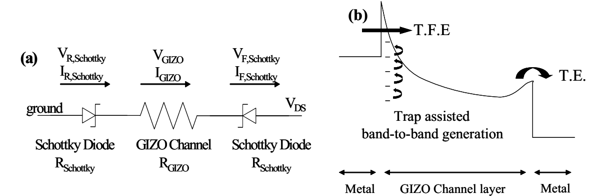

Fig. 3. (a) Equivalent circuit model and (b) Schematic energy band diagram with current mechanisms in MSM structure.

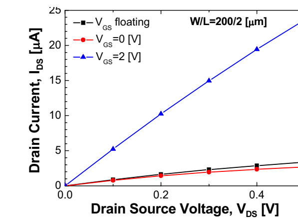

Fig. 4. I_{DS}-V_{DS} curves when the gate electrode is floated and gate voltage is at 0 and 2 [V]

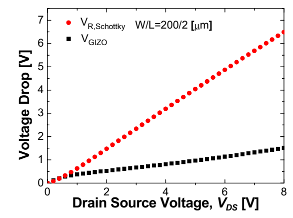

Fig. 5. Voltage drop in channel and contact region calculated using extracted resistance from experimental results.

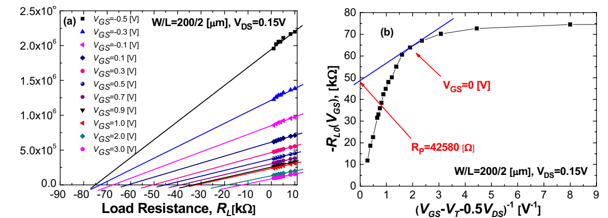

Fig. 6. Gate voltage-dependent contact resistance from (a) $1/I_{DS}$ versus R_L and (b) $-R_{L0}$ versus $1/(V_{GS}$-V_T-$0.5V_{DS})^{-1}$ curve.

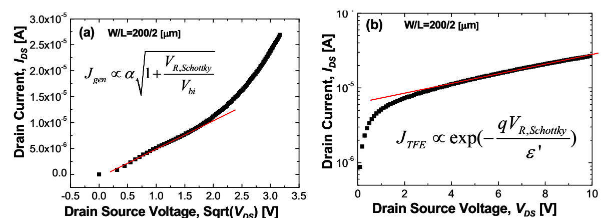

Fig.7. The I_{DS} versus $\sqrt{V_{DS}}$ and V_{DS} curves of MSM structure.

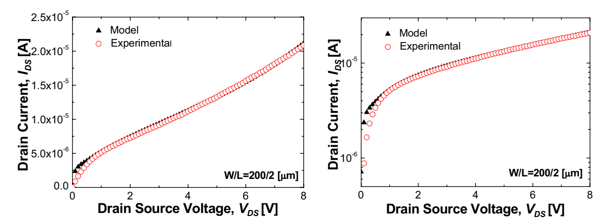

Fig. 8. Measured I_{DS}-V_{DS} characteristics of *a*-GIZO MSM structure compared with the semi-empirical model.

Table I. Used model parameter

Parameter	Value	Parameter	Value
α [A/cm^2]	8.55×10^{-7}	E_B [eV]	0.25
ε_{GIZO}	11.5	N_{sub} [cm^{-3}]	2.0×10^{17}
m_{GIZO}^* [Kg]	0.2 m_o	V_{bi} [V]	0.168